Dear author,

In the stage of preparing your full work for evaluation, after receiving approval of the corresponding abstract, we kindly ask you to follow the next steps:

1. Update your approved abstract (you might want to introduce modifications) and submit it now in a written version according to the abstract template (many abstracts were introduced directly into the websystem). This version of the abstract will compose the *abstracts booklet* to be distributed to the participants when registering;

2. Fill the form in the next page, indicating to which section you would like your work to be directed. This will help organizing the sessions according to the mini-symposia advertised rather than in the areas and subareas present in the websystem. We apologize for this possible confusion. The reason is that we are using the websystem provided by ABCM, which does not allow us to introduce thematic sessions freely.

If any doubts arise, please contact us.

Your presence in MecSol 2017 will help making this a very successful event. We look forward to seeing you in Joinville!

With kind regards,

The Organizing Committee
MecSol 2017

6th International Symposium on Solid Mechanics

Click on the box to select the Mini-Symposia:

☐ Multiaxial and Fretting Fatigue (*Edgar Mamiya* and *Lucival Malcher*);

☐ Composite Materials (*Ricardo de Medeiros*);

☐ Constitutive Models I – Plasticity and Damage (*Lucival Malcher*, *Miguel Vaz Jr.* and *Edgar Mamiya*);

☐ Constitutive Models II – Viscoelastic and Viscoplastic Solids: Models and Applications (*Heraldo Mattos*);

☐ Impact Engineering (*Marcílio Alves*);

☐ Structural Reliability Methods and Reliability-Based Design Optimization (*André Beck*);

☐ Topology Optimization of Multifunctional Materials, Fluids and Structures (*Eduardo Lenz Cardoso* e *Emilio Carlos Nelli Silva*);

☐ Topological Derivatives: Theory and Applications (*André Novotny*);

☐ X-FEM, G-FEM and Meshfree Methods (*Roberto Dalledone Machado* and *Rodrigo Rossi*);

☐ High Order Finite Elements (*Marco Lúcio Bittencourt*);

☐ Nonlinear Analyses (*Eduardo Campello*);

☒ Other section;

MECSOL Joinville 2017

April 26-28, 2017
Joinville, Santa Catarina, Brazil

DYNAMIC AND FATIGUE ANALYSIS: COMPARISON BETWEEN TIME AND FREQUENCY DOMAINS

Juliano Carvalho da Silva Filho, Said Morais Sirio Rocha
Department of Simulation and Structural Analysis
SEMCON
julianocsf@hotmail.com, saidmsrocha@gmail.com

Jorge Alberto Rodriguez Duran, José Flávio Silveira Feiteira
Department of Mechanical Engineering
Universidade Federal Fluminense - EEIMVR

Antonio Carlos Müller, Alencar Nascimento Pinto Filho, Caio de Souza Diniz, Patrícia Rocha Maia, Rômulo Franco Pereira, Uile Pires Borges da Silva
Department of Simulation and Structural Analysis
SEMCON

Priscila Sousa Nilo Mendes
PPGEM
Universidade Federal Fluminense - EEIMVR

ABSTRACT

The improvement of criteria for the durability evaluation is a growing need in the automotive industry and is fundamental for an optimized product development. Often, the structures are submitted to a general dynamic load and analyzed with CAE tools, mainly by the finite element method. This paper discusses about methodologies for dynamic simulations analyses in time and frequency domain to evaluate the fatigue life, and presents a bench test to correlate with simulation results. The evaluate fatigue life in time domain, is determined from stress history in deterministic form, however in frequency domain, is determined by the response PSD (Power Spectral Density) and from spectral moments in the probabilistic form. The methodology has been applied in cantilever beam with a lumped mass in the free end, and exposed to a random unidirectional base excitation. Were realized a bench test with data acquisition of base and response acceleration by accelerometer, and the beam strain by strain gauges. The test data has been applied as input data for the dynamics simulation and its validation. For fatigue analysis the life was estimated by the Palmgren-Miner rule. The method of the load cycle counting is the main difference between time and frequency domain damage analysis. For the cycle counting in time domain the Simplified Rainflow method has been applied, and in frequency domain the cycle counting is presented by stress PDF (Probability Density Function) proposed by Dirlik. Afterwards, the results of fatigue life time achieved by both simulations domain were compared to the bench test result.

Keywords: Vibration, Durability, Random Fatigue, Dynamic Simulation

1 INTRODUTION

The study of the dynamic behavior of a component when subjected a random base excitation contemplates the development of most engineering components. During product development it is important to choose modern and reliable methods that meet the design deadline and enable the design of products with more durability, lighter and cheaper.

This paper discusses methodologies for the dynamic analysis in time and frequency domain that can be used in development of products to predict their durability, fatigue life or damage.

To evaluate the fatigue damage in frequency domain, several methods can be applied. The time domain is based on cycle counting and damage accumulation, such as rainflow count and Palmgren-Miner linear damage rule.

Rahman et al., 2008 [1], Bosco Junior, 2007 [2], Bishop, 1994 [3], and Bishop and Sherratt, 1989 [4], concluded that Dirlik's solution has better correlation with time domain results, and Quigley and Lee, 2012 [5], evaluated the Dirlik solution and concluded that this model is also the best for automotive application, even though the damage can be underestimated by up to 30%.

In 2014 Teixeira, Jones and Draper [6] evaluated both approaches and established some comparisons in terms of accuracy and range of application. In this study, the fatigue life for both domains was close.

This paper is based on bench test and numerical simulations in time and frequency domains, and the damage achieved by physical test is our reference for the comparison between simulations.

In time domain, the maximum and minimum stresses and the number of cycles are determined from the events history. The input data for numerical simulation is the displacements history from the base obtained from acceleration signal measured.

In the frequency domain the numbers of cycles and stresses are determined in probabilistic way from the response PSD (Power Spectral Density) of stress. The input data for numerical simulation in frequency domain is PSD of the acceleration signal measured.

This paper is organized in sections, to gradually introduce the concepts to describe the analysis methodologies. With these concepts, a case study of a beam with a lumped mass on free end, was subjected to a base excitation and was used for comparison of fatigue evaluations.

2 MODAL SUPERPOSITION

The modal superposition method is an approach to calculate the dynamic response of a linear structure. This method solves the equations of motion by uncoupling them in one equation with 1 DOF (degree of freedom) for each vibration mode considered. This solution is more efficient when the numbers of vibration modes is not big.

The deformed structure configuration is the linear combination of responses of each vibration modes. Each mode has its weight or participation factor that shows the relevance of this respective mode in the dynamic response evaluation. Follows the modal superposition equation (1) [7].

$$\{U(t)\} = y_1.\{\emptyset_1\} + y_2.\{\emptyset_2\} + y_3.\{\emptyset_3\} + \cdots + y_n.\{\emptyset_n\} = \sum_{i=1}^{n} y_i(t)\{\emptyset_i\} \quad (1)$$

The participation factor (y_i) can be calculated by the following equation (2) [7].

$$m_i.\ddot{y}_i(t) + c_i\dot{y}_i(t) + k_i y_i(t) = f_i(t)$$

$$\begin{cases} m_i = \{\emptyset_i\}^T.[M].\{\emptyset_i\} & \rightarrow Generalized\ mass \\ c_i = \{\emptyset_i\}^T.[C].\{\emptyset_i\} & \rightarrow Generalized\ damping \\ k = \{\emptyset_i\}^T.[MK].\{\emptyset_i\} & \rightarrow Generalized\ stiffness \\ f_i = \{\emptyset_i\}^T.\{F(t)\} & \rightarrow Generalized\ force \end{cases} \quad (2)$$

3 CONVERSION ACCELERATION TO VELOCITY AND DISPLACEMENT

The signal conversion is a combination of numerical integration and digital filters application. The filters are applied to eliminate the integration constants. Is recommended the application of the high pass filter type FIR (Finite Impulse Response), with the equivalent curve of Chebyshev Type 1, due to this filter don´t generate the signal time delay and presents short transition band [8], [9].

The frequency response and the Impulse response of this filter are shown in the Figure 1.

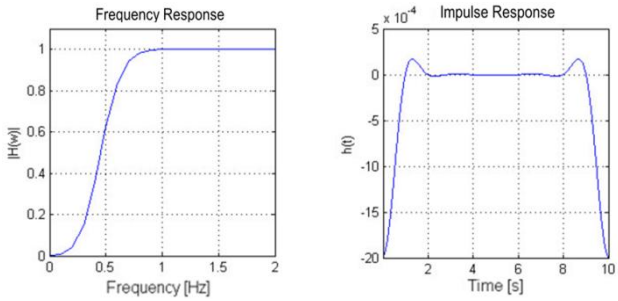

Figure 1: The frequency response and the impulse response for the high pass filter FIR to remove the errors of the numerical integration process [8].

When the signal has an unspecified frequency in the filter is observed the time aliasing problem. This problem causes a distortion in the signal extremes. The length of the affected stretch for this problem is previewed in applied impulse response filter. One way to minimize the length of the affected stretch is to apply a little truncation in the initial and final stretch before the filtering process.

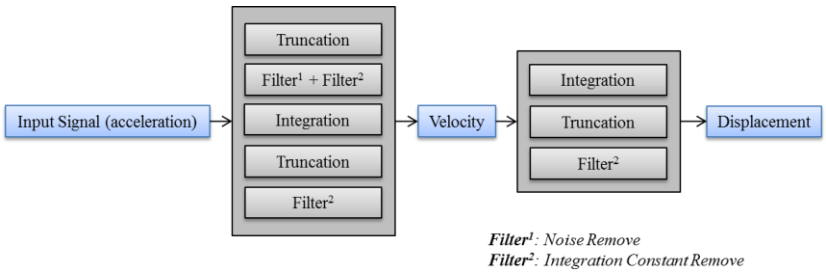

Figure 2: Flowchart to calculate velocity and displacement from acceleration signal without noise, using digital filters to remove integration constants and the truncation to reduce errors due to time aliasing [8].

4 RANDOM ANALYSIS

Random response analysis is used when a structure is subjected to a nondeterministic continuous excitation that is expressed in a statistical sense by a power spectral density (PSD). The application of frequency response techniques to the analysis of random processes requires that the system be linear and that the excitation be stationary with respect to time [10].

The random response procedure uses the set of eigenmodes extracted in a previous eigenfrequency step to calculate the corresponding power spectral densities (PSD) of response variables [11].

The transfer function theorem states that, if $H_{ja}(\omega)$ is the frequency response of any physical variable,u_j, due to an excitation source, Q_a, then u_j can be determined by equation (3) [10].

$$u_j(\omega) = H_{ja}(\omega).Q_a(\omega) \tag{3}$$

Where $u_j(\omega)$ and $Q_a(\omega)$ are the Fourier transforms of u_j and Q_a, then the power spectral density of the response $S_j(\omega)$, is related to the power spectral density of the source, $S_a(\omega)$, by equation (4) [10].

$$S_j(\omega) = \left|H_{ja}(\omega)\right|^2.S_a(\omega) \tag{4}$$

5 PSD AND SPECTRAL MOMENT

Power spectral density (PSD) is the frequency response of a random or periodic signal. The PSD describes the variation of the quadratic mean value of the function in relation to a frequency range. It can be estimated by using the mean square value of a narrow frequency range for several central frequency values and dividing by the frequency band.

The spectral density function $Sxx(\omega)$ can be expressed as the Fourier transform of the auto-correlation function:

$$Sxx(\omega) = \frac{1}{2\pi}\int_{-\infty}^{\infty} Rxx(\tau)e^{-j\omega\tau}d\tau \tag{5}$$

The mean square value is found integrating the PSD function in the frequency domain.

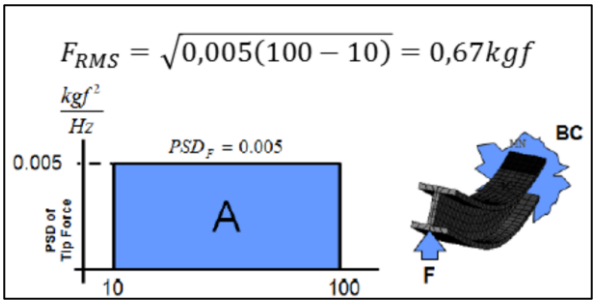

Figure 3: Spectral density function of a load applied on clamped beam [6].

It is possible, from PSD, to perform a statistical evaluation of a random process, such as standard deviation and variance.

Spectral Moment is a property of the PSD and it is a quantitative parameter that describes the characteristic of the signal without need of sample in the time domain [12], [13].

Given the division of the PSD curve into intervals, the moment of order *n* is calculated by the sum of the product of the area of each interval with the respective frequency raised to power *n*.

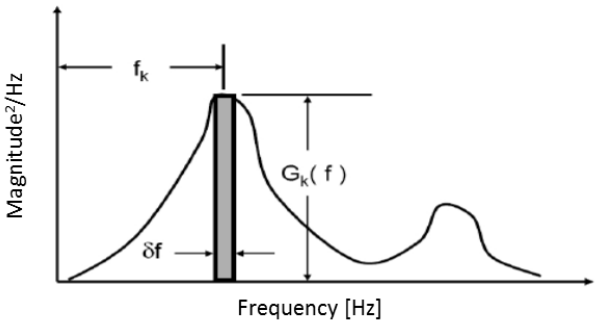

Figure 4: Moments of PSD.

According to Figure 4, the moment of order *n* is mathematically described as:

$$M_n = \sum_{k=1}^{N} f_k{}^n G_k(f).\delta f \tag{6}$$

It is necessary to determine the moments of all orders for a single and complete definition of PSD. However, in practice, only moments m_0, m_1, m_2 and m_4 are sufficient for calculating spectral fatigue by providing relevant information to be used in calculating fatigue life [12], [14].

6 CYCLE COUNTING

6.1 Time Domain

A lot of procedures were investigated and proposed to have a load that represents the same effect of a random loading. After several publications the consensus was that the best procedure was proposed by T. Endo and his collaborators in Japan, called “Rainflow cycle counting” [15].

Also known as "counting cycle in time domain method," Rainflow was the first accepted method to extract the closed cycles. It is indicated when a load sequence (or block) is applied repeatedly.

The simplified method uses three consecutive points in time from a load history to determine if a cycle will be formed. A cycle is formed always that the next single interval is greater or equal to the first simple interval, Figure 5.

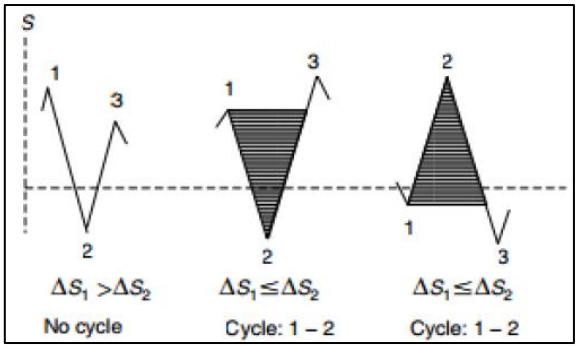

Figure 5: Rainflow simplified method

The norm ASTM E1049-85 (2011) presents the Rainflow counting algorithm. Follow a description of this algorithm:

1- Reorder the load history to initiate from the maximum peak or minimum valley;
2- Reading the next peak or valley. If there are no points to reading, finish;
3- If there are less than three points, return to step 2. Form X and Y amplitudes using the three most recent peaks and valleys that were not been discarded;
4- Compare the values of amplitudes X and Y. If X < Y, return to step 2. If X ≥ Y, go to step 5;
5- Count Y amplitude as a cycle. Discard the peak and the valley of Y and return to step 3.

6.2 Frequency Domain

For a random and stationary data set, the probability of a given data assuming a value at a given time t is known as the probability density function (PDF) [16]. Figure 6 shows a time sample of a random signal where the probability of x (t) assuming a value between x and x + dx in a total time of $(dt_1 + dt_2 + dt_3 + dt_4)$ is given by the equation:

$$P[x \leq X(tb) \leq x + dx] = \frac{dt_1 + dt_2 + dt_3 + dt_4}{T} = f_X(x) = \frac{1}{T}\sum_{i=1}^{k} dt_i \tag{7}$$

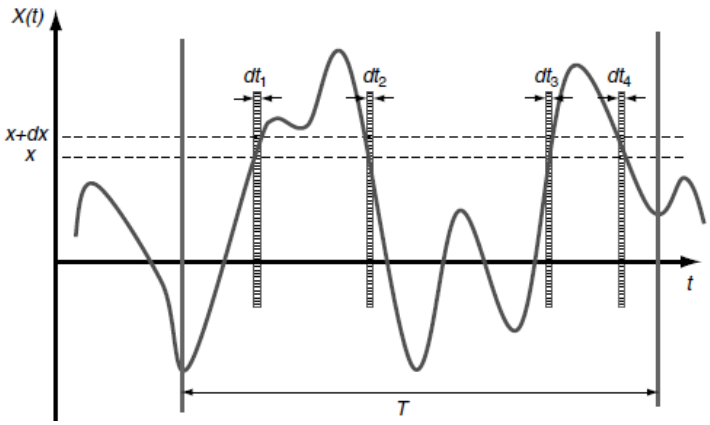

Figure 6: Set of random data in time domain.

The PDF is the main component of the Rainflow method in the frequency domain [17]. It differentiates the various methodologies available and make possible to calculate the damage. Normal or Gaussian distribution, Raileigh distribution, and Dirlik distribution are some of the probability density functions that are applied in each particular case.

The PDF (Probability Density Function) proposed by Dirlik is mathematically described by equation (8) [17], [5].

$$p(S_r) = \frac{1}{2\sqrt{M_0}} \cdot \left[\frac{D_1}{Q} e^{\frac{-z}{Q}} + \frac{D_2 Z}{R^2} e^{\frac{-z^2}{2R^2}} + D_3 Z e^{\frac{-z^2}{2}} \right] \tag{8}$$

Where Table 1 shows parameters resulting from an adjustment procedure performed on the data of the numerical simulations:

Table 1: Parameters of the adjustment procedure of numerical simulations data.

$D_1 = \frac{2(x_m - \gamma^2)}{1+\gamma^2}$	$D_2 = \frac{1 - \gamma - D_1 + {D_1}^2}{1 - R}$	$R = \frac{\gamma - x_m - {D_1}^2}{1 - \gamma - D_1 + {D_1}^2}$	$Z = \frac{S_r}{2\sqrt{M_0}}$
$Q = \frac{1.25(\gamma - D_3 - D_2 R)}{D_1}$	$x_m = \frac{M_1}{M_0}\sqrt{\frac{M_2}{M_4}}$	$\gamma = \frac{E[0]}{E[P]} = \frac{M_2}{\sqrt{M_0 . M_4}}$	$D_3 = 1 - D_2 - D_1$

In this way the number of cycles of S_r is determined by equation (9) [17], [5].

$$N(S_r) = E[P] . T . p(S_r) . \Delta S_r \tag{9}$$

Where:
S_r: Stress range;
$N(S_r)$: Number of cycles of stress range
$E[P] = \frac{M_4}{M_2}$: Expected number of peaks;
T: Exposure time;
$p(S_r)$: Probability Density Function

7 PALMGREN MINER FAILURE CRITERIA

The definition of fatigue damage (D) is a relation between the repetitions number of a constant (n) alternating stress and the necessary number to failure occurrence showed in SN curve (N_f). Fatigue damage is expressed by:

$$D = \frac{n}{Nf} \tag{10}$$

For a sequence of loads, the generated damage for each load is irreversible and cumulative. The Palmgren-Miner damage rule accumulation proposes that the fatigue failure occurs when the sum of the damage generated by each load reaches a critical damage value (D_{PM}). The fatigue failure is expected:

$$\sum D = \sum \frac{n}{Nf} \geq D_{PM} \tag{11}$$

The SN curve presents a limit value of fatigue endurance, however cycles with alternating stress below the fatigue limit can become harmful, if some of the subsequent amplitudes stress exceed the original fatigue limit [17].

To account the negative influence of periodic overloads, the Miner and Miner-Haibach models proposes an extension of SN curve, according Figure 7. In this way, all stress amplitudes accumulate damage [17].

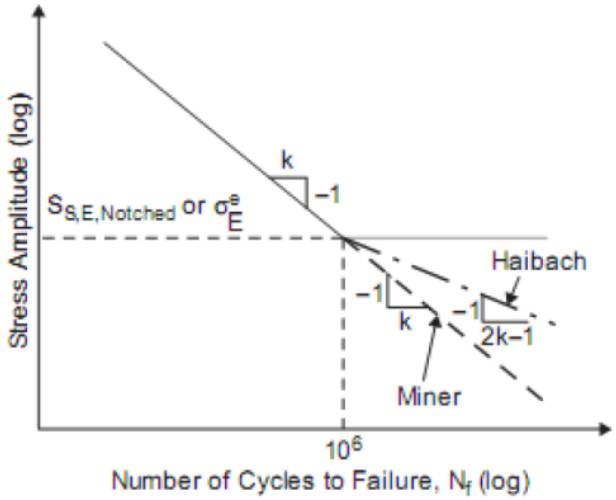

Figure 7: Schematic SN curve with constant amplitude for steel subjected to a load with variable amplitude [17].

8 CASE STUDY

The case study considered was a beam with a lumped mass on its free end subjected to a random base excitation, as shown in Figure 8.

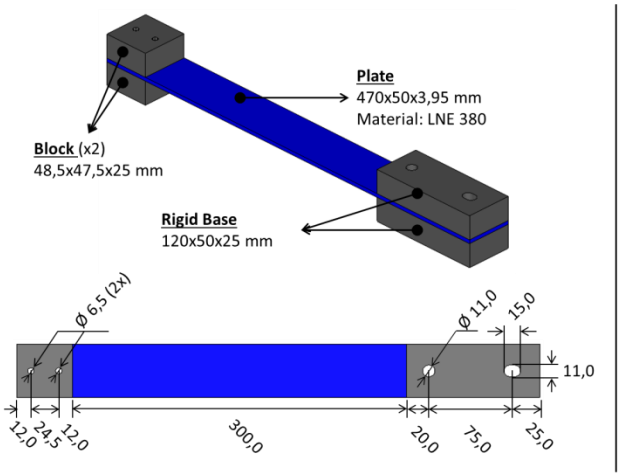

Components	Mass [kg]
Plate	0,693
Block	0,430
Bolt M6	0,015

Figure 8: Case study.

8.1 Equipment Used in Physical Testing

The Table 2 lists the equipment utilized for the random and impact test.

Table 2: Equipment.

	EQUIPMENT	MODEL
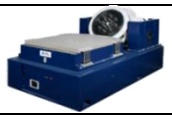	Electrodynamic Shaker	M748A/ GT1000
	Acquisition Hardware	LMS SCADAS mobile 01
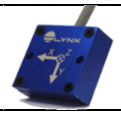	Accelerometer	Lynx ICP-5G
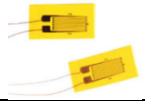	Strain Gage	Excel Sensores: PA-06-125AA-350ENC-3

For the impact test, the base of the beam was fixed on rigid table. A unidirectional strain gauge was placed near the base of the beam (see Figure 9). The excitation was applied through a vertical pulse at the free end of the beam.

For the random test, an accelerometer was added at the base of the beam (which was attached to the shaker). With this accelerometer the random excitation was measured (see Figure 9). In all tests the ‘Acquisition hardware Lynx ADS 2002 AI2164’ was utilized with a 1000Hz data acquisition frequency.

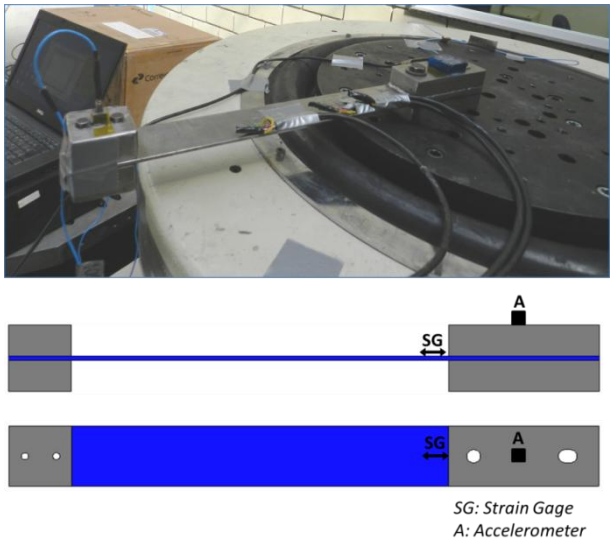

Figure 9: Position of the sensors and assembly for the random test.

8.2 Impact Test

The impact test was conducted to determine the natural frequency and the damping factor. The Figure 10 (a) presents stress over time measured during the test and Figure 10 (b) the PSD of the signal. The maximum value of PSD occurs at the frequency of 10.71Hz. This value represents the natural frequency of the first mode of vibration.

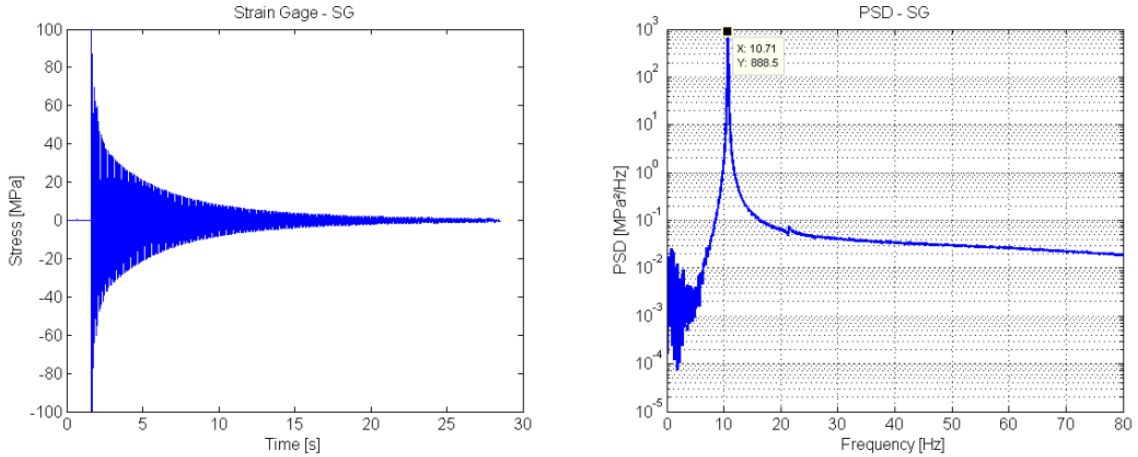

Figure 10: Stress measured during the Impact Test: (a) Stress over time (natural response), (b) PSD of the stress signal.

To determinate the damping factor of the first vibration mode, a fourth-order band-pass Butterworth filter was used. The lower and upper cutoff frequency were set to 5.4Hz and 21.4Hz respectively [18].

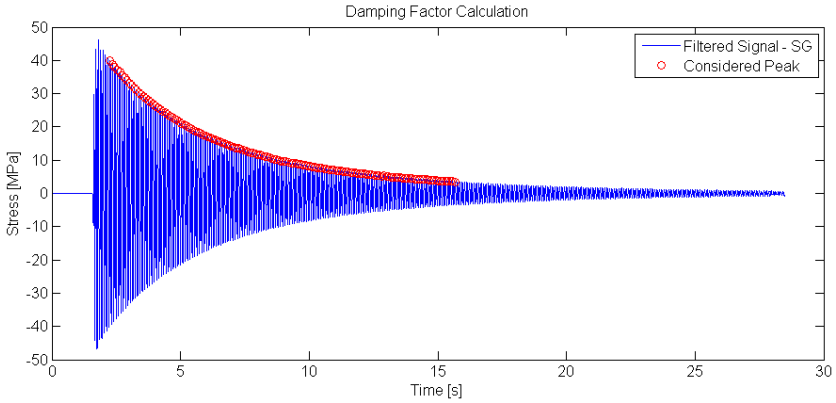

Figure 11: Natural response of the structure for the first mode of vibration (Stress history).

To calculate the damping factor, the adopted methodology was the same methodology adopted at [18]. The mean logarithmic decrement was obtained from 145 peaks consecutives (indicated as red point at Figure 11). With those points the logarithmic decrement was calculated utilizing the equation (12) and the damping factor with equation (13).

$$\delta_{médio} = \frac{1}{C_2^n} * \left[\sum_{i=1}^{n} \sum_{j=i+1}^{n} \frac{1}{(j-i)} ln\left(\frac{A_i}{A_j}\right) \right] = 0{,}0166 \tag{12}$$

$$\zeta = \frac{1}{\sqrt{1 + (2\pi/\delta_{\text{médio}})^2}} = 0{,}26\% \tag{13}$$

8.3 Random Test

The random test was conducted in order to excite the beam transversally whit a PSD signal, that is equivalent to the PSD of an acceleration signal measured at the frame of a real vehicle. The acceleration signal shown in Figure 12 (a) was measured on the chassis of a heavy commercial vehicle traveling on a rough road. The PSD of this signal, presented in Figure 12 (b), was utilized as input to the shaker, which reproduces it between 2 and 80Hz on a random signal for 20 sec.

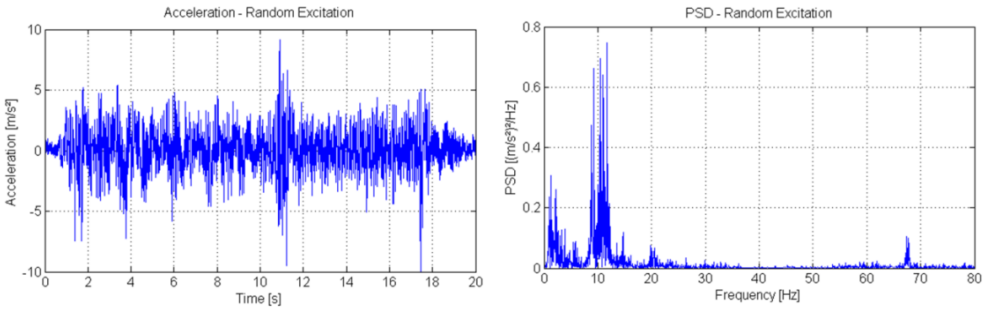

Figure 12: Random acceleration signal considered for shaker reproduction: (a) Signal history, (b) Signal PSD.

8.4 Finit Element Model

The pre and post-processing was made in the HyperMesh 13.0 and the processing on the OptiStruct 13.0 solver.

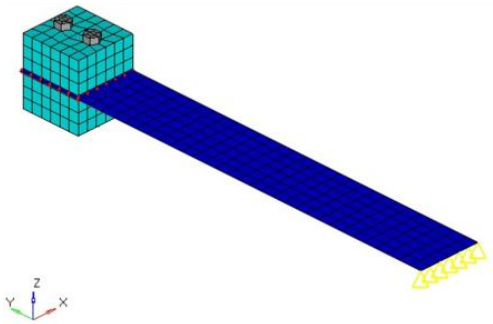

Figure 13: Finite element model.

The Figure 13 presents the finite element model. The plate was modeled with shell elements "CQUAD4" type, with an average size of 10 mm, the blocks and bolts were both modeled with a solid "CHEXA" element type, with an average size of 10 mm. The connection between the block and plate was realized out node by node, with rigid element "RBE2" type. The nodes that are in the intersection surface between the bolt and block were modeled to be coincident, to represent bolt junction.

The goal of the numeric analyses of finite elements is to know the dynamic response of the beam for the applied excitation, therefore it results in the necessary data for the durability analyses of the component.

In the time domain, the excitation applied is the displacement history of the beam base, and the dynamic response of interest is the stress history on the beam.

In the frequency domain the applied excitation is not the displacement history. Actually, it is the PSD of the acceleration signal, and the result obtained is the stress PSD at the beam.

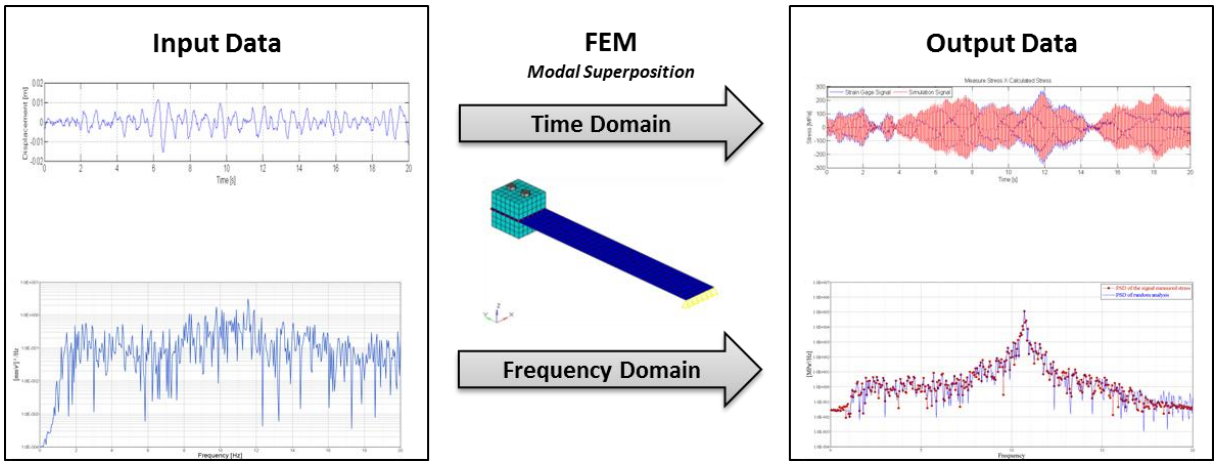

Figure 14: Simulation: time domain x frequency domain.

8.5 Dynamic Simulation - Time Domain

This study uses the "Modal Transient Response" analysis, which utilizes the modal superposition method to define the dynamic response. Only the first vibration mode of the beam was considered to compose its dynamic response, due to the natural frequency of the second vibration mode being higher than maximum excitation frequency set in the shaker, which is 80Hz. The method considered for the modal analysis was the Lanczos method.

In the time domain dynamic simulation, the load considered was defined by the displacement history on the beam base. This displacement was obtained through the conversion of the acceleration signal measured in the random test [18].

The conversion of acceleration signal in displacement was realized with the process defined in the item 3. The high and low pass filters that were used to remove the offsets and the noise are shown in the Figure 15.

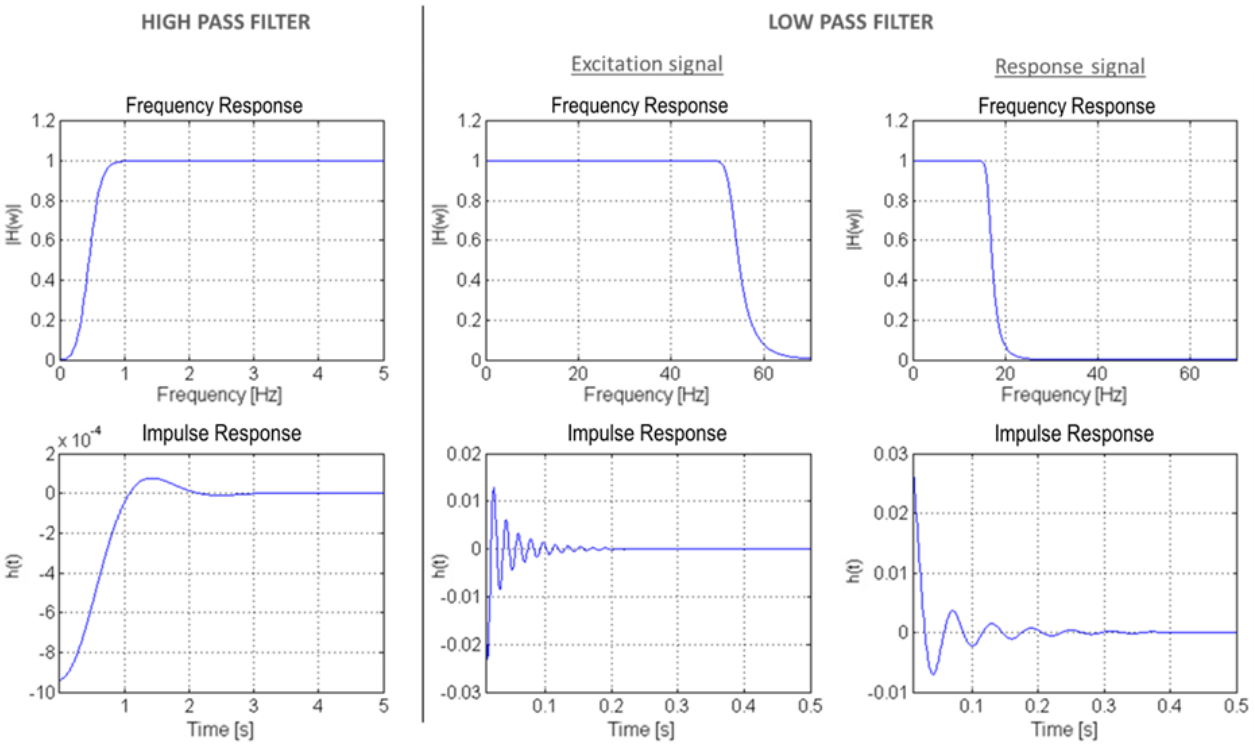

Figure 15: The frequency response and the impulse response of the FIR high pass and low pass filters designed to remove the offsets and the noise of the acceleration signal.

The acceleration signals measured, as well velocity and displacement signals converted are shown in the Figure 16.

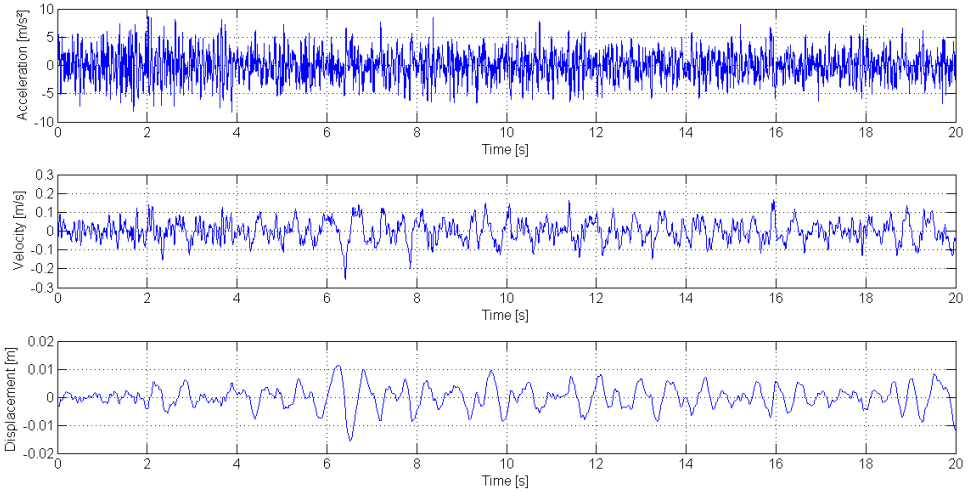

Figure 16: Base acceleration, velocity and displacement signals.

The Figure 17 illustrate the comparison between the measured stress and calculated stress with the stress historical obtained at the time domain dynamic simulation. In the higher graphic the signals are compared in their essences, while the lower graphic shows the comparison of the two envelope curve of the positive peak. As observed, the correlation between the measured and calculated stress is excellent.

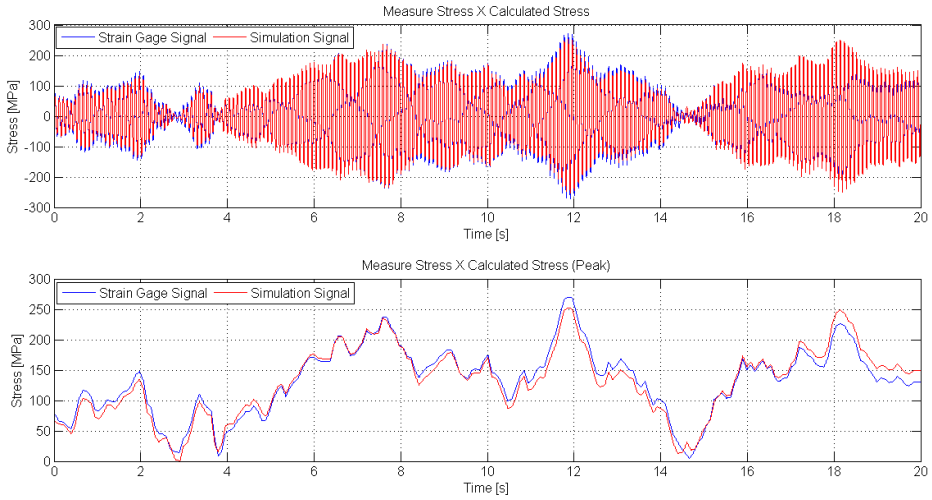

Figure 17: Comparison between the measured and calculated stress through the time domain simulation: (a) Full Signal, (b) Positive envelope curves.

8.6 Dynamic Simulation - Frequency Domain

The first step in random analysis is to calculate the frequency response function (FRF) for unitary excitation that, in this case, is in the vertical direction.

In the random analysis the frequency range of interest was determined from 1 to 20 Hz. The Figure 18 shows the frequency response of stress for the instrumented point. The damping factor was considered ($\zeta = 0{,}26\%$).

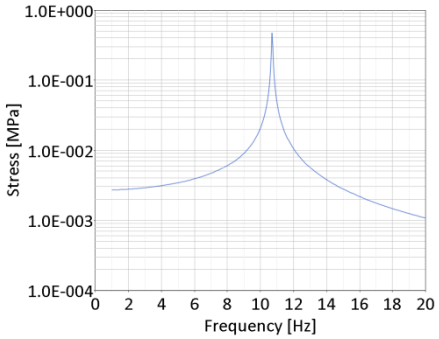

Figure 18: Frequency response of stress for the instrumented point

The PSD of the base acceleration shown in the Figure 19 was considered as input data for the random analysis.

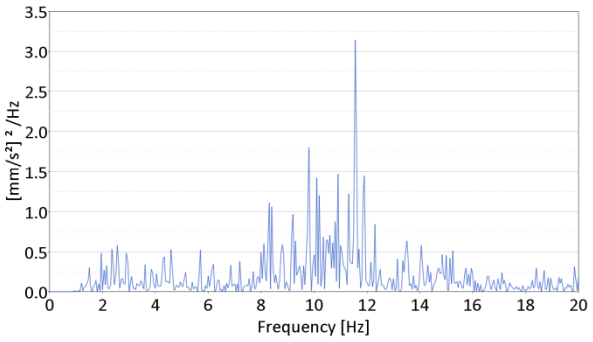

Figure 19: PSD of base acceleration

The PSD of stress determined in the random analysis and by the signal measured at the same point are shown in Figure 20.

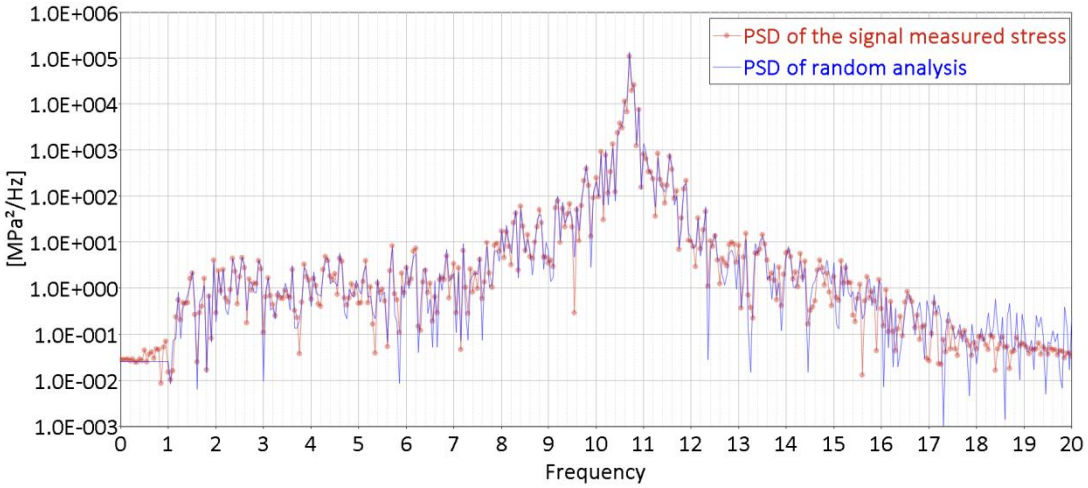

Figure 20: PSD of stress determined in the random analysis and by the signal measured.

8.7 Fatigue Evaluation

The fatigue evaluation was divided into three steps. In the first step, the fatigue curve of the material was estimated and the factors of reliability and surface finishing were considered. The second step presents the cycle count. For the time domain the simplified rainflow methodology presented in item 6.1 was used; in the frequency domain the cycle count was extracted from the PDF proposed by Dirlik as presented in item 6.2. Finally, the accumulated damage for each analysis was determined according to the Palmgren-Miner linear damage hypothesis presented in item 7.

The scripts used for counting cycles and fatigue evaluation in both domains were developed in Matlab®.

- **Fatigue Curve**

The material of the beam is a steel ABNT NBR 6656 LNE 380, and the estimated fatigue curve is shown in Figure 21. As the Miner's rule was considered, the material fatigue limit was not considered.

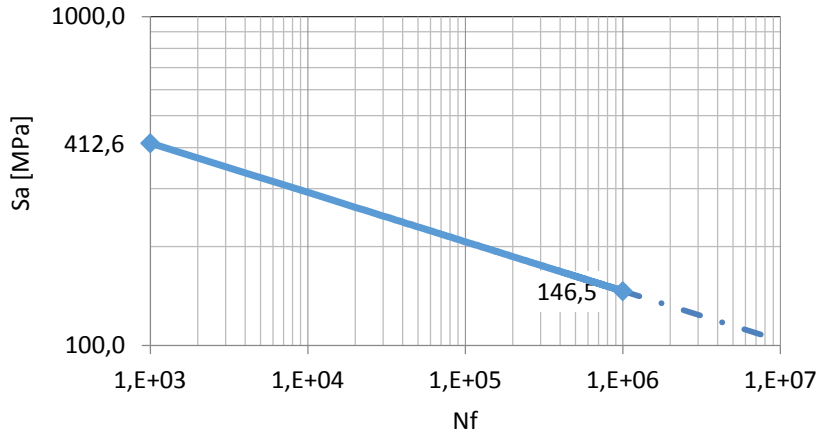

Figure 21: S-N curve

Equation (14) is derived from the fatigue curve, Figure 21.

$$N_f = \left(\frac{S_a}{1162.3}\right)^{-0.15} \tag{14}$$

- **Cycle counting**

The cycle counting technique is the main difference between the time and frequency domain fatigue approach.

For the application of the simplified rainflow counting technique the stress signal in the time domain was divided into 120 classes. The calculated rainflow matrix and range pair for the measured stress and the calculated stress in the transient analysis are shown in the Figure 22.

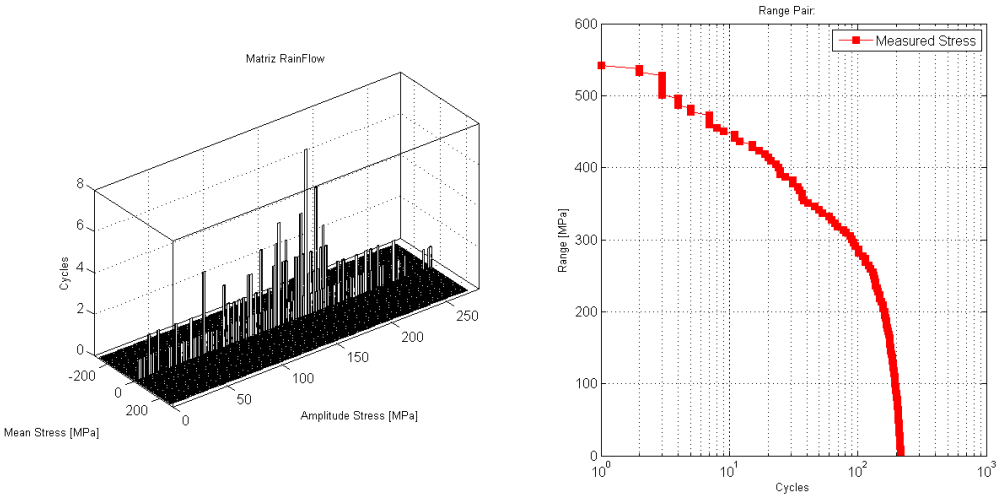

Figure 22: Rainflow and Range Pair of measured stress

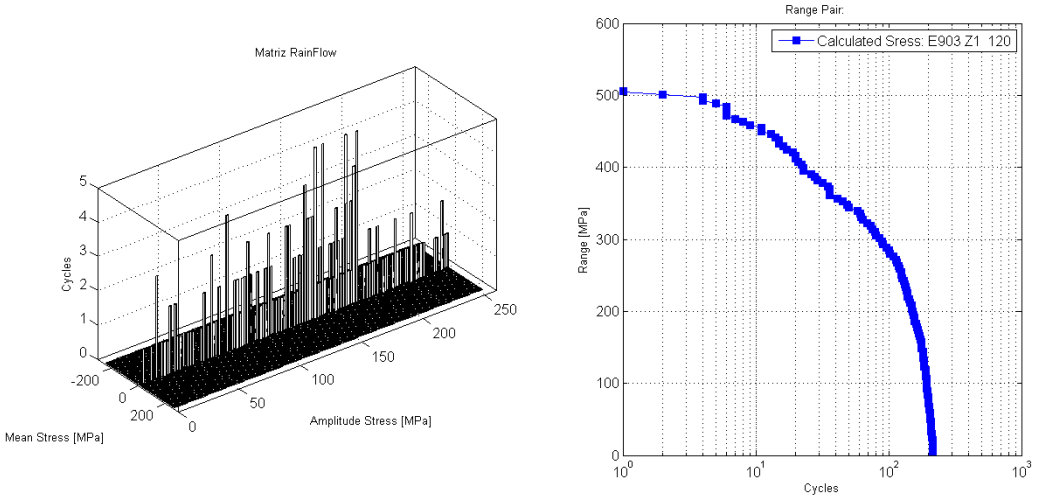

Figure 23: Rainflow and Range Pair of calculated stress in time domain

For the fatigue analysis in the frequency domain, the probability density function proposed by Dirlik and its respective range pair for time of 20 seconds are shown in Figure 24. The range pair is determined by the PDF, however, there must be an upper limit to the integration process. This threshold value is defined as cutoff stress, which is the maximum stress range that can presumably be found in stress history. For this analysis, the adopted cutoff stress was the maximum range determined in the measured stress (540 MPa).

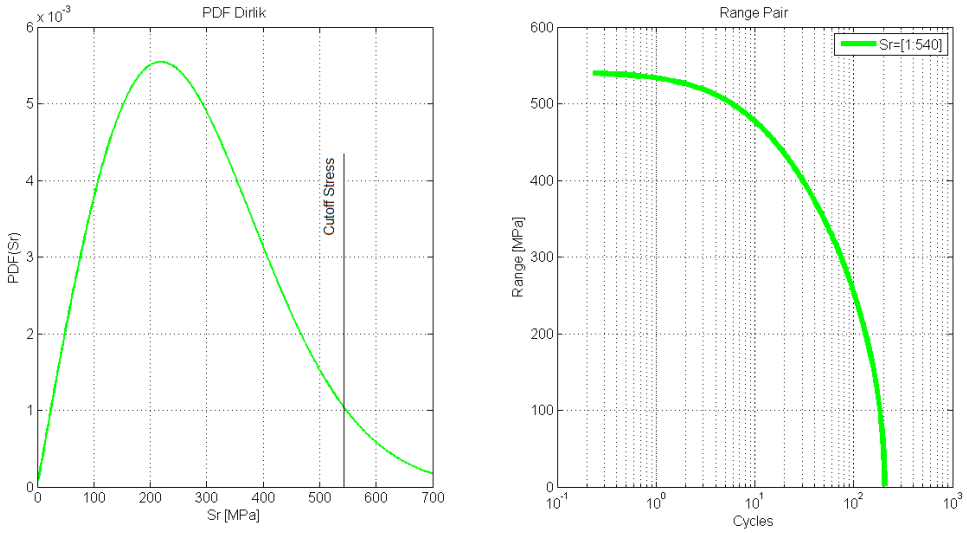

Figure 24: PDF and Range Pair of calculated stress in frequency domain

The Figure 25 shows the range pair for the measured stress and the calculated stress for both domains.

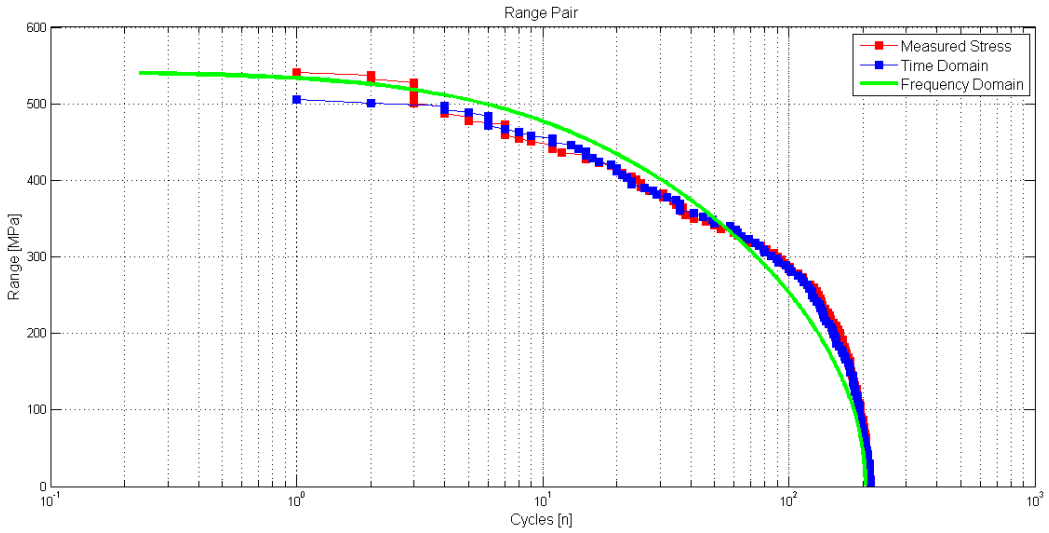

Figure 25: Range Pair for the measured and calculated stress in time and frequency domain

- **Fatigue Life Evaluation**

The accumulated damage and fatigue life expected for the beam in each case evaluated is presented in the Table 3.

Table 3: Fatigue Life Evaluation

Fatigue Evaluation	**Measured Stress**	**Simulation**	
		Time Domain	**Frequency Domain**
Damage	9.53E-04	8.88E-04	1.19E-03
Life [h]	5.8	6.3	4.7

9 CONCLUSION

The fatigue analysis based in the time domain simulation have shown a life 9% higher than the estimated life calculated considering the stress history measured. The life calculated in the frequency domain predicted a life 19% shorter.

In the time domain there is the advantage of analyzing the stress history, and also the maximum values. However the computational cost is extremely higher than analyses in the frequency domain.

In the frequency domain there is the difficulty to set the cutoff value for the stress to determine the range pair from the PDF. During the execution of this experiment it was easy, because we had access to the measured stresses, but this may not be the case in every situation.

The influence of the mean stress over the fatigue resistance is not considered at the applied methodology for the frequency domain, because the mean stress expected for the random vibration is zero.

REFERENCES

[1] Rahmann, M. M. et al., 2008, Fatigue Life Prediction of Two-Stroke Free Piston Engine Mounting Using Frequency Response Approach, Vol. 22 No. 4. Pp. 480-493, European Journal of Scientific Research.

[2] Bosco Junior, R., 2007, Análise Numérico-Experimental de Componentes Sujeitos à Fadiga Por Solicitações Aleatórias – Avaliação de Modelos, Dissertação de Mestrado, Universidade Federal de Santa Catarina, Florianópolis.

[3] Bishop, N. W. M., 1994, Spectral methods for estimating the integrity of structural components subjected to random loading. Handbook of fatigue crack propagation in metallic structures, v. II, p. 1685-1720, New York.

[4] Bishop, N. W. M.; Sherratt, F., 1989, Fatigue life prediction from power spectral density data. Part 2: Recent development. Environmental Engineering, v. II, p. 5-10.

[5] Quigley, J. e Lee, Y., 2012, Assessing Dirlik´s Fatigue Damage Estimation Method for Automotive Applications, SAE Int. J. Passeng, Cars – Mech. Syst.

[6] TEIXEIRA, G. M.; JONES, D.; DRAPER, J. Randon Vibration Fatigue - A study comparing time domain frequency domain approaches for automotive applications. SAE Technical paper series, 2014.

[7] Avelino, A. F., 2012, Elementos Finitos a base da Tecnologia CAE – Análise Dinâmica, Cápitulos 3 e 4, 2ª ed. Érica Ltda, São Paulo.

[8] Rocha, S. M. S.; Feiteira, J. F. S.; Mendes, P. S. N.; da Silva, U. P. B.; Pereira, R. F., June 2016, "Method to Measure Displacement and Velocity from Acceleration Signals", Int. Journal of Engineering Research and Application, ISSN: 2248-9622, Vol.6, Issue 6, (Part-4), pp. 52-59.

[9] Ribeiro, J., 1999, Algoritmo Para Medir Deslocamento em Grandes Estruturas a partir de Sinais Acelerômetros, Tese de Doutorado, Departamento de Engenharia Mecânica, Pontifícia Universidade Católica (PUC) do Rio de Janeiro, Rio de Janeiro.

[10] MSC Nastran Dynamic Analysis User's Guide, 2012, Cap. 8

[11] Abaqus 6.13 User's Guide Volume II: Analysis.

[12] Bishop, N. W. M. e Aherratt, F., 2000, Finite Element Based Fatigue Calculations, The International Association for the Engineering Analysis Community, Farnham, United Kingdon.

[13] Nieslony, A., 2010, Comparison of Some Selected Multiaxial Fatigue Failure Criteria Dedicated for Spectral Method, 48,1 pp. 233-254, Journal of Theoretical and Applied Mechanics, Warsaw.

[14] Bishop, N. W. M., 1999, Vibration Fatigue Analysis in the Finite Element Environment, XVI Encuentro Del Grupo Español De Fractura, Espanha.

[15] Dowling, N. E.; 2007, Mechanical Behavior of Materials: Engineering Methods for Deformation, Fracture and Fatigue, 3ª Edição, Cap. 9, Pearson Prentice Hall

[16] Newland, D. E., 1993, An introduction to Random Vibrations, Spectral and Wavelet Analysis, John Wiley & Sons, New York.

[17] Lee, Y.-L.; Barkey, M. E.; Hong-Tae, K.; 2011, Metal fatigue analysis handbook: practical problem-solving techniques for computer-aided engineering, Cap. 9, [S.l.]: Elsevier.

[18] Rocha, S. M. S., 2016, Metodologia para simulação dinâmica de uma estrutura submetida a uma excitação de base randômica obtida a partir de acelerômetros, Dissertação de Mestrado, Programa de Pós-graduação de Engenharia Mecânica (PPGMEC), Universidade Federal Fluminense (UFF), Volta Redonda.